Available online at www.sciencedirect.com
ScienceDirect
International Journal of Heat and Fluid Flow 28 (2007) 1136–1143
International Journal of HEAT AND FLUID FLOW
www.elsevier.com/locate/ijhff

Numerical analysis of shock wave interaction with a cloud of particles in a channel with bends

Pawel Kosinski *

The University of Bergen, Department of Physics and Technology, Allegaten 55, 5007 Bergen, Norway

Received 7 August 2006; received in revised form 4 November 2006; accepted 9 November 2006
Available online 23 January 2007

Abstract

Shock wave interactions with a cloud of particles were analysed using an Eulerian–Lagrangian numerical technique. In this approach, the particle–particle and particle–wall interactions can be modelled directly. Simulations were carried out in a channel with two bends: an issue important for pneumatic and slurry transport of particles, as well as for dust explosions in industrial facilities. At the beginning, the results are shown as snapshots, showing the reader how the particle cloud propagates through the channel. At the next stage some statistics is performed in order to analyse the influence of channel geometry. The following parameters are analysed: the history of the percentage of particles that have travelled along the whole channel and the history of the average kinetic energy of the particles. It is shown how the channel structure and particle diameter influences the parameters.

Keywords: Shock waves; Particle/fluid flows; Numerical simulation; Particle transport; Dust explosions

1. Introduction

1.1. Overview of recent literature

In literature there are a few dozen publications devoted to the topic of shock wave interaction with a cloud of particles, sometimes in domains with complex geometry. Applications range from dust explosions in coal mines and grain elevators, to solid propellant combustion in rocket engines. Both experimental and numerical simulation techniques have been used in these publications and detailed analyses of shock wave and particle behaviour have been performed. Here a few papers are mentioned as examples illustrating a general trend.

Wang et al. (2001) present numerical simulations of shock wave behaviour in the presence of a square cavity filled with particles. The authors state that investigation of shock wave interaction with both obstacles and particles is important for understanding complex phenomena, such as dust explosions in industrial facilities. The simulation is in a two-dimensional domain, and the gas is assumed to be inviscid. The simulation is performed both for pure gas and the gas with particles, and a detailed comparison is made. The authors emphasize that numerical simulations of such processes may be a research tool, which is superior to experiments. Experiments are often complex and not easy to repeat. The same has been mentioned in many other papers as well.

Park and Baek (2003) perform simulations of the interaction of a shock wave with a cloud of carbon particles that either undergo combustion or are inert. Additionally, a wedge is located in the computational domain to make the process more complex and thus more real. The combustion is modelled as a simple one-step heterogeneous reaction between carbon and oxygen.

Igra et al. (2004) analyse shock wave reflection from a wedge where the whole domain is filled with a dusty gas. Different solids loadings and particle diameters are considered. This paper differs from other works where only part of the computational domain is filled with dust, often near

* Tel.: +47 55 58 28 17; fax: +47 55 58 94 40.
E-mail address: Pawel.Kosinski@ift.uib.no

0142-727X/$ - see front matter © 2006 Elsevier Inc. All rights reserved.
doi:10.1016/j.ijheatfluidflow.2006.11.003

the wedge. In the latter type of simulations, the shock wave initially propagates in a pure gas and later interacts with a particle cloud, giving rise to an extra phenomenon, namely reflection of the wave from the cloud, and this phenomenon Igra et al. try to avoid.

Boiko et al. (1997) pay special attention to the drag force coefficient. They point to the well-known fact that, in spite of great number of data in literature, this coefficient is only well determined as a function of the Reynolds number and only for a single particle. The Mach number needs to be taken into account for high relative velocities, as does the particle concentration for flows with high concentration. In the first part of their paper, Boiko et al. present some experimental results, where the value of the drag force coefficient is determined, and later they use this in numerical simulations. The results of computation are validated against experiments.

A complex and interesting problem is the interaction of a shock wave with a layer of particles. Since the boundary layer is turbulent, the vortex structures scoop dust out of the bed of particles and the dust is then entrained up and over the vortex structures and is then transported by the turbulent flow. This was shown, e.g. by Kuhl et al. (1989) and Collins et al. (1994). Another explanation is the particle–particle interactions (Kosinski et al., 2005; Kosinski and Hoffmann, 2006).

In Klemens et al. (2001), results of simulations are presented where the geometry of a real channel with fixtures and fittings is mimicked by including vertical obstacles. The interphase interaction is described by simple relations for drag force and convective heat exchange, and additionally the Magnus lift force is implemented. In the paper particle–particle interactions are not taken into account, even though such interactions are likely to dominate for the high particle concentrations present in dust layers.

Kosinski et al. (2005) compare two numerical techniques: Eulerian–Eulerian and Eulerian–Lagrangian. The former has been frequently used for analysis of dust lifting behind shock wave, in spite of the fact that modelling of particle–particle and particle–wall collisions may be questionable using this approach. Therefore Kosinski et al. suggest using the Eulerian–Lagrangian technique and they show that this leads to superior results. Also in Kosinski and Hoffmann (2005) a similar issue is addressed.

Rogue et al. (1998) study experimentally and numerically the interaction of a shock wave with a bed of particles. The bed is situated in a vertical tube and fluidization is induced by a shock wave travelling from the bottom of the tube forcing the particles to move upwards. Very detailed experimental analysis is performed, where the dust bed consists of one, two and more layers of particles. Thanks to that, different phenomena could be included or excluded in the numerical simulations (e.g. collisions that are not important for only one layer). Rogue et al. also experimentally determine the drag force coefficient, which they later use for their numerical investigation. Finally, the numerical results are compared with the experiments.

Also an interesting problem is the interaction with a dust layer, where the chemical reaction between the particles and an oxidiser in the gas, is taken into account. This has been especially emphasized in works: Fedorov and Gosteev (2002), Gosteev and Fedorov (2003), Fedorov and Fedorchenko (2005). See also works: Rose et al. (1999, 2000).

The problem of shock wave propagation in a channel becomes complex, when the channel is not straight but consists of bends and obstacles. This process is even more challenging to analyse when the flow is two-phase. The solid particles are subject to the interaction with the flowing gas, as described in detail in the papers mentioned above, but also with channel walls. This is of importance for studying pneumatic or slurry of particles, but also for such issues like dust explosions. Especially for modelling of dust explosions, the problem of particle–particle and particle–wall interactions is often neglected in order to simplify the computer code and the analysis process. Nevertheless, in the author's previous paper: Kosinski (2006) a problem of dust mixture propagation in a branched channel is described. Two simulation techniques are compared there: Eulerian–Eulerian and Eulerian–Lagrangian. It is shown that modelling particle–wall collisions is crucial when the channel geometry is complex.

In this paper the following problem is considered: propagation of dust mixture in a channel with two bends after having interacted with a shock wave. The Eulerian–Lagrangian modelling technique is used in order to investigate such processes. The results are shown as snapshots, showing the reader how the particle cloud propagates through the channel, but also some statistics is performed in order to analyse the influence of channel geometry and particle size.

1.2. Simulation technique

Two techniques are generally used for simulating two-phase flow phenomena: Eulerian–Eulerian (E–E) and Eulerian–Lagrangian (E–L) (see e.g. Crowe et al., 1998).

In the E–E approach both phases are treated as separate fluids, coupled by, for instance, drag force and heat exchange. This approach is computationally economical and suitable for dense mixtures with two-way coupling, but it requires good phenomenological models, usually based on kinetic theories for granular flows. It is especially challenging to implement phenomena like particle–particle and particle–wall interactions, even though attempts at doing this have been reported in literature.

In the E–L approach, the particles are tracked in the computational domain and in this aspect this kind of model is more physically correct. Also, it is much straightforward to implement phenomena such as particle–particle and particle–wall interactions, as well as some particle-fluid interactions, such as lift forces.

The objective of this paper is to perform simulations of the interaction of a shock wave with a cloud of particles in a channel with two bends using the E–L approach.

2. Mathematical model

The complete mathematical model consists of three parts:

– description of the gas phase behaviour,
– description of the solid phase behaviour,
– modelling of interphase mechanisms.

The model is given below (subscript g refers to the gas phase), starting with the equations for the gas phase (two-dimensional case), which include some terms describing the interphase interaction:

$$\frac{\partial \rho_g}{\partial t} + \frac{\partial \rho_g u_x}{\partial x} + \frac{\partial \rho_g u_y}{\partial y} = 0 \tag{1}$$

$$\frac{\partial \rho_g u_x}{\partial t} + \frac{\partial \rho_g u_x^2 + p}{\partial x} + \frac{\partial \rho_g u_x u_y}{\partial y} = -f_x \tag{2}$$

$$\frac{\partial \rho_g u_y}{\partial t} + \frac{\partial \rho_g u_x u_y}{\partial x} + \frac{\partial \rho_g u_y^2 + p}{\partial y} = -f_y \tag{3}$$

$$\frac{\partial E_g}{\partial t} + \frac{\partial u_x(E_g + p)}{\partial x} + \frac{\partial u_y(E_g + p)}{\partial y} = -f_x v_x - f_y v_y - Q \tag{4}$$

$$\frac{p}{\rho_g} = RT_g \tag{5}$$

The parameters are: ρ is the bulk density; u_x, u_y are the x- and y-components of the velocity of the gas phase; v_x, v_y are the x- and y-components of the velocity of the solid phase; p is the pressure; R is the individual gas constant; T is the temperature; E is the total energy; Q is the heat exchange rate between the phases; f_x, f_y are the x- and y-components of interphase forces.

The total energy per unit volume of the gas phase is written as

$$E_g = \rho_g \frac{u_x^2 + u_y^2}{2} + T_g \rho_g c_V \tag{6}$$

In the equations the interphase interactions are

– $\vec{f} = \vec{f}_{drag}$ is the drag force,
– Q is the heat transfer rate.

The basic formula for the drag force may be written in the following way:

$$\vec{f}_{drag} = n \frac{\pi d^2}{8} C_D \rho_g |\vec{u} - \vec{v}|(\vec{u} - \vec{v}) \tag{7}$$

where $\vec{u}$, $\vec{v}$ are the velocity vectors of the gas and the solid phase, respectively; d is the diameter of the particles and n is the particle number density.

The value of the drag coefficient C_D is primarily a function of the Reynolds number, defined as

$$Re = \frac{\rho_g d|\vec{u} - \vec{v}|}{\mu} \tag{8}$$

And one of the empirical formulas that can be used is (e.g. Khasainov et al., 2005):

$$C_D = \frac{24}{Re}[1 + 0.183\sqrt{Re}] + 0.42 \tag{9}$$

Due to a difference in temperature between the phases, heat exchange should be taken into account as well. It was assumed that only the convective heat transfer takes place; no other mechanisms were considered:

$$Q = n\pi d \lambda Nu(T_g - T_p) \tag{10}$$

where Nu is the Nusselt number with the following formula:

$$Nu = 2 + 0.6\sqrt{Re}Pr^{1/3} \tag{11}$$

where Pr is Prandtl number.

As mentioned above, the E–L approach treats the particles as points, whose motion is the result of the interaction with the moving gas. The biggest drawback of the method is the fact that in real industrial applications the number of the particles is too large to consider the behaviour of all of them. In order to overcome the problem, a number of particles are often "pooled" to form "virtual particles", so that the number of the particles to be considered can be reduced. For small geometries with a limited number of particles, the E–L type of model can be used accurately without introducing virtual particles and this was done in the present research.

The model for the solid phase is (the set of equations must be written for all the particles and $i = 1, \ldots,$ number of particles):

$$m_i \frac{dv_{xi}}{dt} = f_{ix} \tag{12}$$

$$m_i \frac{dv_{yi}}{dt} = f_{iy} \tag{13}$$

$$\frac{dT_i}{dt} = \frac{1}{m_i c_S} Q_i \tag{14}$$

$$I_i \frac{d\omega_i}{dt} = M_i \tag{15}$$

where for ith particle: m_i, I_i are the mass and the moment of inertia, respectively; T_i is the temperature; v_{xi}, v_{yi} are the components of velocities; ω_i is the angular velocity (z-component); f_{ix}, f_{iy} are the x- and y-components of force acting on ith particle due to interphase forces and collisions; Q_i is the heat transfer rate between the particle and the surrounding fluid; M_i is the torque acting on the particle due to collisions and due to shear stress distribution on the particle surface.

The expressions for the drag force, as well as the heat exchange rate, are the same as described in Eqs. (7) and (10). The only difference is the absence of parameter n, describing the number of particles per unit volume (the

number density), since the expressions in this case are written for a single particle.

Thus the force acting on the gas phase is modelled as

$$\vec{f} = \sum_j \vec{f}_j$$

where $\vec{f}_j$ describes the action of all individual particles in a computational cell.

For computing of the drag force, the velocity of the particle surrounding gas is needed. Since the gas velocities are stored in the cells centres and the particles location may freely change, one needs to know the exact value of the gas velocity at the point of the particle location. This is done by the linear interpolation. It must be noted that also other techniques were tested, where the order of the interpolation was increased, but this did not lead to better results in this research.

Also it must be emphasized that the amount of angular momentum of the particle is trivial compared to its linear momentum, especially for fast processes. On the other hand the angular velocity of particles must be modelled, since this is of importance for modelling collisions. Therefore the torque acting on the particle (Eq. (15)) may be considered as negligible.

In this research, the body forces (i.e. gravity) were excluded from the model. The reason is that for fast processes, the gravity can be safely neglected: for the data used in this research, the drag force was of order of magnitude 10^{-7}, whereas the gravity force can be estimated to be of order 10^{-9}. One has to remember, however, that for large tunnel heights this issue might become important.

The E–L approach makes it possible to take into account collisions between the particles. In this research, the hard sphere model was adopted. Its detailed description may be found, for example, in Crowe et al. (1998). In this model we neglect the particle deformation, and assume that the friction, μ_c, on sliding particles obeys Coulomb law. Additionally a coefficient of restitution, e, is defined as a ratio of the post-collisional to the pre-collisional velocity components perpendicular to the plane of the impact. Both coefficients are specified and are constant. The collisions of the particles with the walls are also easily included in the model in an analogous manner.

3. Numerical method

3.1. The flow of the gas phase

The calculations were carried out on a uniform mesh with square cells. Additionally a layer of "ghost" cells was implemented on each boundary. Eqs. (1)–(4) can all be represented in the following way (see e.g. Toro, 1999):

$$\frac{\partial \overline{U}}{\partial t} + \frac{\partial \overline{F}}{\partial x} + \frac{\partial \overline{G}}{\partial y} = \overline{S} \tag{16}$$

where $\overline{U}$ is a vector of conserved variables; $\overline{F}$, $\overline{G}$ are vectors containing convective fluxes and $\overline{S}$ is a vector containing source terms. The dimension of the vectors is thus equal to four for a two-dimensional flow of a two-phase mixture. As an example the vector $\overline{U}$ is

$$\overline{U} = [\rho_g, \rho_g u_x, \rho_g u_y, E_g]^T \tag{17}$$

The process of computation may be split into two stages:

(1) The free flow of gas without any interaction with the particles; the step is described by

$$\frac{\partial \overline{U}}{\partial t} + \frac{\partial \overline{F}}{\partial x} + \frac{\partial \overline{G}}{\partial y} = \overline{0} \tag{18}$$

(2) The flow of the particles. This step is described in Section 3.2.

(3) The interaction between the phases that results in changing of the parameters of the both phases (the bulk density, velocity and temperature); the step is described by

$$\frac{\partial \overline{U}}{\partial t} = \overline{S} \tag{19}$$

The first group of Eqs. (19) was solved using the Godunov-type MUSCL Hancock partial differential solver (Toro, 1999):

$$\overline{U}_{jk}^{\tilde{n}+1} = \overline{U}_{jk}^{\tilde{n}} + \frac{\Delta t}{\Delta x}\left[\overline{F}_{j-\frac{1}{2},k}^{\tilde{n}} - \overline{F}_{j+\frac{1}{2},j}^{\tilde{n}}\right] + \frac{\Delta t}{\Delta y}\left[\overline{G}_{j,k-\frac{1}{2}}^{\tilde{n}} - \overline{G}_{j,k+\frac{1}{2}}^{\tilde{n}}\right] \tag{20}$$

for: $j = 1, \ldots, nx$; $k = 1, \ldots, ny$; $\tilde{n}$ is a number of the current time step.

The fluxes were calculated by the exact solution of the Riemann problem. The boundary conditions were of two types:

– the solid wall at the bottom and top of the computational domain,
– the open wall at the left and right hand sides.

The boundary conditions at the solid wall were as follows:

$$u_{xo} = -u_{xA}; \quad u_{yo} = -u_{yA}; \quad \rho_o = \rho_A; \quad T_o = T_A \tag{21}$$

whereas at the open wall:

$$u_{xo} = u_{xA}; \quad u_{yo} = u_{yA}; \quad \rho_o = \rho_A; \quad T_o = T_A \tag{22}$$

where subscript o denotes a parameter in a "ghost" cell, and A in a cell adjacent to the "ghost" one.

The equations describing the interactions between the phases constitute a system of ordinary differential equations. In this research they were solved using the VODE solver (see Brown et al., 1989).

3.2. The flow of the particles

The motion of the particles was tracked on the computational domain by solving Eqs. (12)–(15) that constitute a

system of ordinary differential equations. They may be written in the same form as (19) and were solved using the aforementioned VODE solver.

Eqs. (12)–(15) were solved in each time step and new values of particle parameters: the linear velocity, the angular velocity and the temperature were found. Having the linear velocity made it possible to find the new position of each particle.

When two particles were in such a position that they were colliding (i.e. the distance between their surfaces was lower than or equal to zero), a set of procedures was called based on the hard-sphere model. This led to updated values of the linear and the angular velocities.

4. Results and testing

In this work, the following case was considered: a cloud of particles was exposed to a shock wave travelling from the left in a rectangular channel. The shape of the channel and the location and the size of the particle cloud are shown in Fig. 1. The computational domain was split into 384×256 square cells. The length L in Fig. 1 corresponds to number of cells equal to 64, whereas dimension H varied for different cases. It was equal to L, $2 \times L$ or $3 \times L$.

Two particle diameters were considered: $D = \Delta/2$ and $D = \Delta/4$, where Δ is the computational cell size. The particle material density was: $\rho_s/\rho_{g,init} = 769$, where $\rho_{g,init}$ is the initial density of the gas in the channel.

The Mach number of the shock wave was 1.5. The wave was generated by putting a high-pressure section at the inlet of the channel as the initial condition. This wall was simulated as "open", thus the boundary conditions given in (22) were adopted. The outlet was modelled in the same way. The lower and the upper wall, as well as the obstacles walls were modelled using the boundary conditions from (21).

The exact values of the collision parameters are not easy to estimate, and their empirical quantification requires good experimental techniques and observations. According to, e.g. Goldschmidt et al. (2001), the restitution coefficient, e, should be close to 1.0 and therefore the value 0.9 we chose for this research. According to Goldschmidt et al. a good estimate for the friction factor, μ_c, is 0.15.

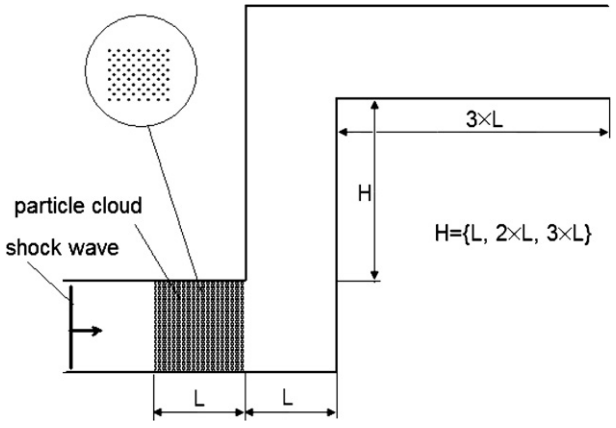

Fig. 1. The initial configuration.

In order to better illustrate the whole process, some results are at first shown for one case corresponding to the value of the parameter H equal to L and particle diameter equal to $\Delta/2$. Four snapshots of particle location for different points in time are shown in Fig. 2. When the shock wave interacts with the cloud, the particles are pushed to the right, which leads to an increase in their concentration (Fig. 2a). At the next stage, the particles collide with the opposite wall and rebounce (Fig. 2b). During this process, they lose some of their kinetic energy: this is dependent on the value of restitution coefficient. Simultaneously their angular velocity rapidly increases: previous changes are due to the shear stress acting on the particles and some particle–particle interactions, but they were of no importance at this stage.

After the collision with the wall, the particles are further pushed upwards by the main stream of the gas, which leads to subsequent collisions with the walls at the top and on the left (Fig. 2c and d). During this interesting period, some particles are pushed to the right by the streaming gas, but a high fraction of them is actually pushed back downwards due to interactions with the walls and a vortex created behind the first bend. In order to illustrate this phenomenon better, Fig. 3a and b shows velocity fields after 2 ms of the gas and of the particles, respectively. In Fig. 3a the vortex, which is pushing particles backwards, is clearly seen. The main stream of the gas is responsible for transport of the particles. Fig. 3b shows somewhat chaotic motion of the particles, even though this movement is determined by the channel geometry, particles distribution and their velocities. The backward movement of the particles can be seen as well. It was observed that some particles have a tendency of coming back to the beginning of the whole channel. This was especially more evident for $H = L$ than for $H = 3 \times L$.

Since various cases were considered in this research, a comparison between them was made. The first set of results is shown in Fig. 4 as a percentage of number of particles that have left the whole channel after 2 ms. The first conclusion is that particles of smaller diameter need less time to travel along the channel, which is the result of their smaller mass and hence their momentum response time is also smaller. This is an obvious conclusion, more interesting is the influence of the parameter H describing the height of the vertical pipe. When this parameter is increased, the number of particles leaving the channel is smaller. We cannot, however, observe a linear trend: the decrease in number of particles leaving the channel is more obvious for smaller values of H parameter. In this research, the maximal H was equal to $3 \times L$, but we can anticipate that for high values of H, the decrease would be much less visible.

At the next stage, the history of the average specific kinetic energy of the particles was analysed for various

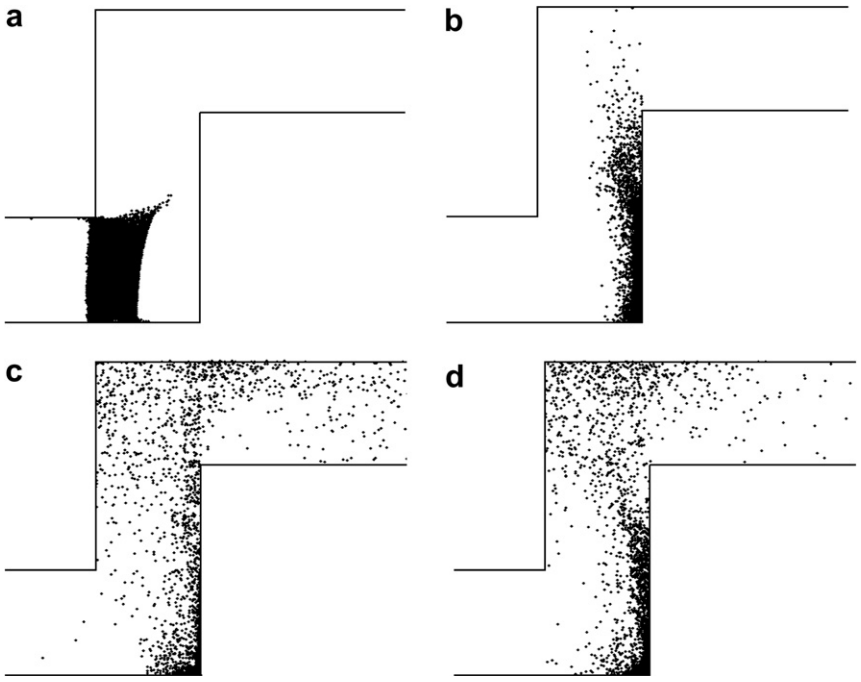

Fig. 2. Snapshots for particle distribution for different points in time: (a) 0.5, (b) 1.0, (c) 1.5 and (d) 2.0 ms. Parameter H is L, particle diameter is $\Delta/2$.

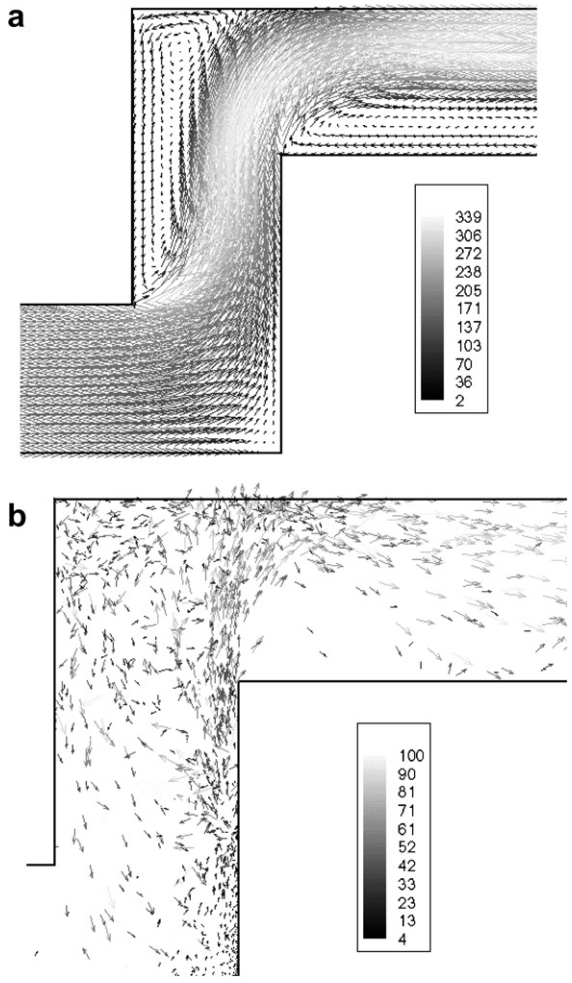

Fig. 3. Snapshot of gas (a) and particle (b) velocity field after 2.0 ms. Parameter H is L, particle diameter is $\Delta/2$.

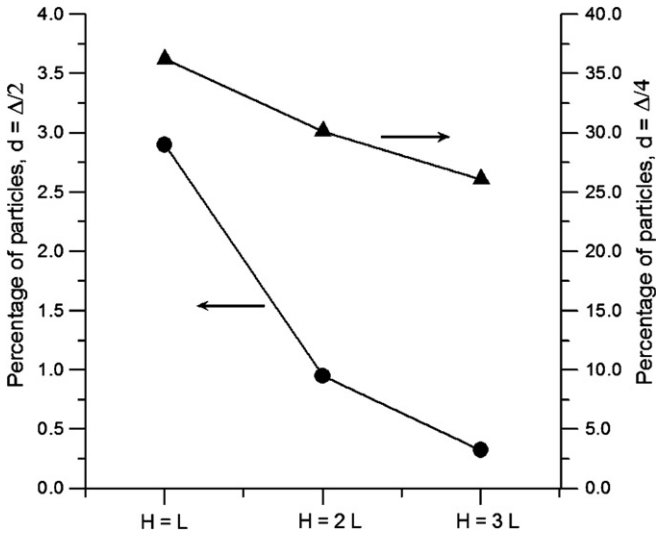

Fig. 4. Percentage of particles that have left the channel after 2 ms.

cases. An example is shown in Fig. 5 where the specific kinetic energy (denoted as E) is made non-dimensional, where the scale is the initial specific kinetic energy of the gas stream (denoted as E_o).

At the beginning the kinetic energy of the particles increases due to interaction with the moving gas behind the initial shock wave. This increase continues until point A on the graph. At this point in time, the particles collide with the wall and hence they lose some of the energy. The minimum value of the energy is at point B. After this, the particles begin to move upwards and they accelerate due to the streaming gas. Around point C they collide with the upper and the left wall in the vertical section of the

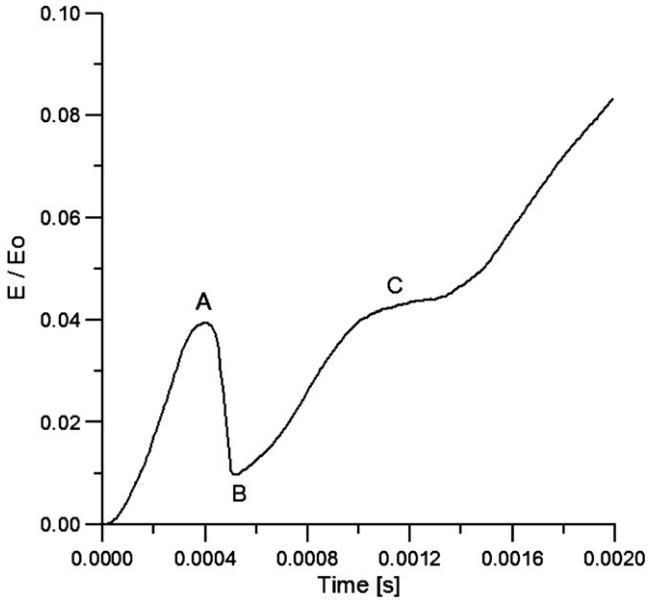

Fig. 5. History of non-dimensional mean energy of particles for $H = 3 \times L$ and particle diameter $\Delta/4$. Explanation of the graph.

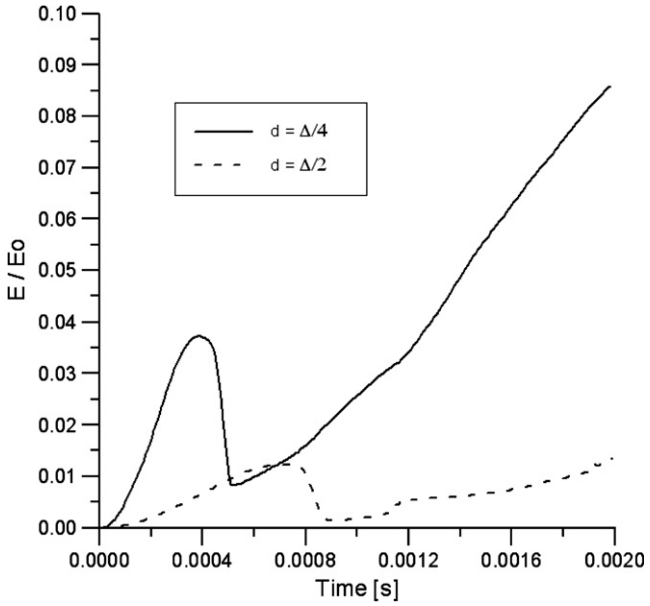

Fig. 7. Histories of non-dimensional mean energy of particles for $H = L$ and two particle diameters: $\Delta/4$ and $\Delta/2$.

channel. The increase of the kinetic energy slows down then, but not crucially: most of the particles are gaining a lot of kinetic energy from the stream and this trend prevails.

Figs. 6 and 7 show histories of the specific kinetic energy for all the cases mentioned above, where both parameter H and particle diameter varied.

Fig. 6 compares the influence of height of the vertical pipe H. All the three curves in this graph correspond to the same particle diameter equal to $\Delta/4$. The most interesting observation is the fact that the height H does not influence crucially the value of specific kinetic energy of the particles. There are, however, differences during the first collision (the equivalent of point A in Fig. 5), as well as during the acceleration prior to collision with the top wall: higher values of the specific kinetic energy are obtained for lower values of H.

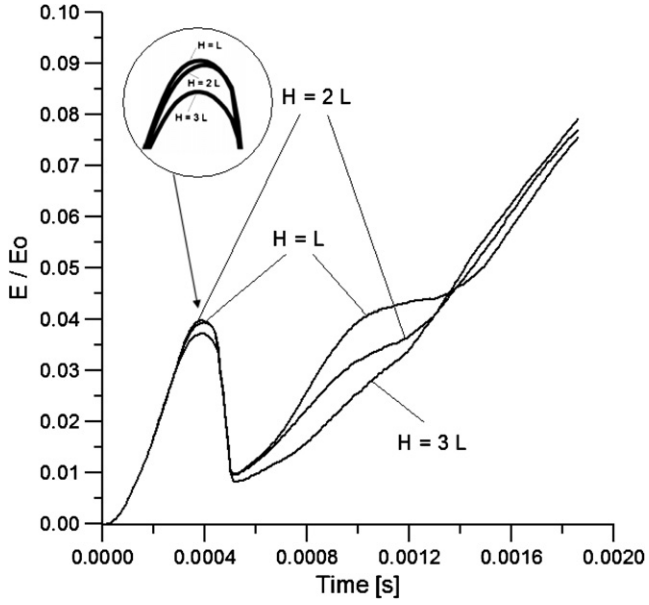

Fig. 6. Histories of non-dimensional mean energy of particles for particle diameter $\Delta/4$.

Fig. 7 compares the influence of particle diameter for the value $H = L$. As one can expect, the lower particle diameter results in much higher kinetic energy, for instance the maximum energy before the first collision is around 3 times higher for particles of diameter $\Delta/4$ than for particles of diameter $\Delta/2$. During the first collision, the bigger particles lose more energy than the smaller particles. After the collision, they carry about 8.8 kinetic energy less than before. For the smaller particles, the value is equal to 4.5, which is about 50% of the former.

The model and the computational code were examined by thorough checking its convergence for grid-independence. The behaviour of the gas phase was convergent to the finest grids, whereas the behaviour of the particulate phase was more complex: the convergence was also observed, however too intense decreasing of the spatial step leads to divergent results. The reason is that when the particle diameter becomes too large in comparison with the cell size, errors occur due to improper modelling of the gas flow around the particles. This was not observed for so-called one-way coupling (only the gaseous phase influences the solid phase, but not the opposite): here the convergence was to the finest grid again. The same issue was also discussed by other researchers. In this research, the two-way coupling approach (both phases influence each other) was used and thus the particle cell size, mentioned above, was chosen as optimal.

An interesting problem is turbulence transport of particles. According to Crowe et al. (1998), small particles tend to follow the fluid motion and they may disperse as fluid elements. On the other hand, large particles will not be affected by the turbulence pulsations. In this paper, the following Stokes number can be defined:

$$St = \frac{\tau_V \Delta u}{l} \tag{23}$$

where τ_V is the particle momentum response time, l is the size of the turbulent structure and Δu is the velocity difference across the shear layer. According to the data in this paper, the value of the Stokes number is greater than one. This suggests that the particles move essentially independently and are not influences by small vorticies.

The computer code was also validated against experiments. Some examples are shown in the author's previous paper: Kosinski and Hoffmann (2006).

5. Concluding remarks

The case of a shock wave interacting with a cloud of particles in a channel with two bends was analysed using the Eulerian–Lagrangian numerical technique. Confined gas–particle flows are frequently found in industrial processes. For flows in channels with complex geometry, such as branched channels or channels with obstacles, the dust cloud may collide with the walls and the obstacles. When modelling such processes, collisions should not be neglected. This was the case in this research, where the particles were a subject to frequent collisions with the walls. Modelling of these processes made it possible to resolve the complex phenomena present during transport of solid particles in a channel with bends. In this paper, it was shown that the collisions lead to an unexpected behaviour of the particles. Therefore this issue cannot be neglected for modelling such processes.

The shape of the bent channel has an influence on particle kinetic energy. Frequent collisions with the walls lead to the loss of the energy. Nevertheless, the height of the bend, H, is not of importance here.

It must be emphasized that particles are not spherical in most cases. Moreover, the coefficient of restitution is not constant and may be a function of, for example, the angle of impact. These issues, already mentioned by some researchers, require fundamental studies.

Another problem is turbulence, which is inherent to nearly all flows in nature and industry. The presence of solid particles in the carrier phase is known to cause turbulence modulation. According to experiments and numerical simulations, a general trend may be observed: small particles tend to attenuate the turbulence, while large particles may enhance turbulence, at least on specific scales. No universal turbulence model taking into account these effects has, however, been proposed.

References

Boiko, V.M., Kiselev, V.P., Kiselev, S.P., Papyrin, A.N., Poplavsky, S.V., Fomin, V.M., 1997. Shock wave interaction with a cloud of particles. Shock Waves 7, 275–285.

Brown, P.N., Byrne, G.D., Hindmarsh, A.C., 1989. VODE: A variable coefficient ODE solver. SIAM Journal on Scientific and Statistical Computing 10 (5), 1038–1051.

Collins, J.P., Fergusson, J.P., Chien, K.Y., Kuhl, A.L., Krispin, J., Glaz, H.M., 1994. Simulation of shock-induced dusty gas flows using various models. AIAA-1994-2309, 25th Fluid Dynamics Conference, Colorado, Springs, 1994.

Crowe, C., Sommerfeld, M., Tsuji, Y., 1998. Multiphase flows with droplets and particles. CRC Press LLC.

Fedorov, A., Gosteev, Y.A., 2002. Quantitative description of lifting and ignition of organic fuel dusts in shock waves. Journal de Physique IV 12, 89–95.

Fedorov, A.V., Fedorchenko, I.A., 2005. Computation of dust lifting behind a shock wave sliding along the layer verification of the model. Combustion Explosion and Shock Waves 41, 336–345.

Goldschmidt, M.J.V., Kuipers, J.A.M., Van Swaaij, W.P.M., 2001. Hydrodynamic modelling of dense gas-fluidised beds using the kinetic theory of granular flow: effect of coefficient of restitution on bed dynamics. Chemical Engineering Science 56, 571–578.

Gosteev, Y.A., Fedorov, A.V., 2003. Mathematical simulation of lifting and ignition of particles in coal deposits. Combustion Explosion and Shock Waves 39, 177–184.

Igra, O., Hu, G., Falcovitz, J., Wang, B.Y., 2004. Shock wave reflection from a wedge in a dusty gas. International Journal of Multiphase Flow 30, 1139–1169.

Khasainov, B., Kuhl, A., Victorov, S., Neuwald, P., 2005. Model of non-premixed combustion of aluminium-air mixtures, 14th APS Topical Conference on Shock Compression of Condensed Matter, Baltimore, MD, July 31–August 5.

Klemens, R., Kosinski, P., Wolanski, P., Korobeinikov, V.P., Markov, V.V., Menshov, I.S., Semenov, I.V., 2001. Numerical study of dust lifting in channel with vertical obstacles. Journal of Loss Prevention in the Process Industries 14, 469–473.

Kosinski, P., 2006. On shock wave propagation in a branched channel with obstacles. Shock Waves 15 (1), 13–20.

Kosinski, P., Hoffmann, A.C., 2005. Modelling of dust lifting using the Lagrangian approach. International Journal of Multiphase Flow 31 (10–11), 1097–1115.

Kosinski, P., Hoffmann, A.C., 2006. An investigation of the consequences of primary dust explosions in interconnected vessels. Journal of Hazardous Materials 137 (2), 752–761.

Kosinski, P., Hoffmann, A.C., Klemens, R., 2005. Dust lifting behind shock waves: comparison of two modelling techniques. Chemical Engineering Science 60 (19), 5219–5230.

Kuhl, A.L., Chien, K.Y., Fergusson, R.E., Glowacki, W.J., Collins, P., Glaz, H.M., Colella, P., 1989. Dust scouring by a turbulent boundary layer behind a shock. Archivum Combustionis 9 (1/4), 139–147.

Park, J.S., Baek, S.W., 2003. Interaction of a moving shock wave with a two-phase reacting medium. International Journal of Heat and Mass Transfer 46, 4717–4732.

Rogue, X., Rodriguez, J.G., Haas, F., Saurel, R., 1998. Experimental and numerical investigation of the shock-induced fluidization of a particle bed. Shock Waves 8, 29–45.

Rose, M., Roth, P., Frolov, S.M., Neuhaus, M.G., 1999. Modelling of turbulent gas/particle combustion by a Lagrangian PDF method. Combustion Science and Technology 149, 95–113.

Rose, M., Roth, P., Frolov, S.M., 2000. Modelling of a turbulent reacting gas/particle flow. Acta Mechanica 145, 45–63.

Toro, E.F., 1999. Riemann Solvers and Numerical Methods for Fluid Dynamics. Springer-Verlag.

Wang, B.Y., Wu, Q.S., Wang, C., Igra, O., Falcovitz, J., 2001. Shock wave diffraction by a square cavity filled with dusty gas. Shock Waves 11, 7–14.